Reconstruction in Atom Probe Tomography Considering the Cone Angle of Needle-Like Shaped Samples and Evaluation of Reliability*

Tsuyoshi Yukawa[†]
Institute of Industrial Science, The University of Tokyo,
Komaba 4-6-1, Meguro-ku, Tokyo 153-8505, Japan

Masato Morita
Institute of Industrial Science, The University of Tokyo,
Komaba 4-6-1, Meguro-ku, Tokyo 153-8505, Japan, and
Research Fellow, Japan Society for the Promotion of Science, Japan

Masanobu Karasawa
Institute of Industrial Science, The University of Tokyo,
Komaba 4-6-1, Meguro-ku, Tokyo 153-8505, Japan

Satoshi Ishimura, Norihito Mayama, and Hiroshi Uchida
Physical Analysis Technology Center, Toshiba Nanoanalysis Corporation,
Shinsugita-cho 8, Isogo-ku, Yokohama 235-8522, Japan

Yoko Kawamura and Kohei M. Itoh
School of Fundamental Science and Technology, Keio University,
3-14-1 Hiyoshi, Kohoku-ku, Yokohama 223-8522, Japan

Masanori Owari
Environmental Science Center, The University of Tokyo,
Hongo 7-3-1, Bunkyo-ku, Tokyo 113-0033, Japan, and
Institute of Industrial Science, The University of Tokyo,
Komaba 4-6-1, Meguro-ku, Tokyo 153-8505, Japan

The present reconstruction method of Atom Probe Tomography (APT) has the problem that the parameter, in particular the shank angle which represents the region the signal of APT is detectable, is adjusted according to the internal length reference of the sample. The reliable APT reconstruction image could not be obtained in the sample without the reference. We propose the method to calculate the value of the shank angle from the shape of sample and the geometric position relationship between the sample and the detector. We compared the APT reconstruction image in this method to the image in the conventional method with the sample of Si isotope superlattice. The result is that APT 3D image by the new method was reconstructed equivalently to the image by the conventional method. [DOI: 10.1380/ejssnt.2015.235]

Keywords: Atom probe tomography; APT; Reconstruction method; Superlattices; Silicon; Nano-scale imaging, measurement, and manipulation technology

I. INTRODUCTION

Many small electric materials and semiconductor materials are used in electrical products typified by smartphones. Recently, electronic devices and semiconductor devices such as transistors have become smaller and more complex due to rapid progress in nanotechnology and even some of these devices come to be controlled by an atom [1]. In these circumstances, development of the new reliable analytical method which can analyze elements sensitively in smaller region than popular analytical methods is expected in the industrial world [2].

Atom probe tomography (APT) is the unique analytical method which can analyze and evaluate elements and get spatial information for each atom [3]. After a sample is shaped to the needle-like shape by the focused ion beam (FIB), the sample obtains energy needed to ionize the apex atoms by applying high voltage. Then, in the order from the apex of the sample, atoms are emitted as ions with the principle of field evaporation and reach a delay line detector. Spatial information is obtained by arrival positions of ions on the detector. And elemental information is obtained by mass spectrometry using time-of-flight to the detector. Atomic distribution can be obtained by constructing 3D image from these information. At present, not only metals but also semiconductors can be measured by introduction of pulsed laser by APT [4, 5].

APT is the unique analytical method in terms of the ability to measure the materials that cannot be measured by other methods [6]. However, APT has some problems as a practical analysis method. One of the problems is uncertainty of parameters using in reconstruction of APT 3D image. APT reconstruction requires not only the two pieces of information obtained by APT measurement, mass information and position information of the

---

FIG. 1. The relationship between the shank angle and the half cone angle of the needle-like shaped sample.

II. GEOMETRIC MODEL

In APT, field evaporated ions go to the detector according to electric field. Spatial information is obtained by the ions reaching the detector, so atoms in the outer edge of the needle-like shaped sample cannot be detected because they go out of the detector. The region detectable with APT is decided by the rod of the needle-like shaped sample near the central axis, the "shank". The diameter of the rod "shank" is larger as depth of the sample is deeper because radius of curvature of the sample is larger. "Shank angle" is defined as the half cone angle of the shank. Then, we focused on the relationship between the shank angle and the half cone angle of the needle-like shaped sample. Figure 1 shows the relationship between the shank angle, the half cone angle of the sample and the detector. The following relationship (1) exists in this model. Here, s is tangent of the complementary angle of the shank angle, a is the radius of the detector, b is the distance between the apex of the needle-like shaped sample and the detector, and c is the tangent of the complementary angle of the half cone angle of the sample :

$$s = -\frac{b}{a} + \frac{\sqrt{a^2 + b^2}}{a}\sqrt{c^2 + 1} \qquad (1)$$

where s is calculated by the parameters obtained from instruments, a and b, and the parameter obtained from SEM or TEM image, c. It is the shank angle calculated from s, not adjusted by the character samples have, that is used by the APT reconstruction in this study. We compared the APT reconstruction image in this method to the image in the conventional method.

III. EXPERIMENTAL

In this study, Si isotopic superlattice was used as the sample. 10 nm thickness ^{28}Si layers and 20 nm thickness ^{30}Si layers are alternately stacked [9, 10]. Mass numbers of two layers of Si isotopic superlattice are different, so ^{28}Si layers can be distinguished from ^{30}Si layers. Moreover, energies which are necessary for field evaporation are the same at anywhere in Si isotopic superlattice because the two layers are chemically equivalent. The Si isotopic superlattice is almost an ideal sample because artifacts introduced by the multilayer structures is minimized [11]. Many kinds of evaluation in APT such as mass resolution were done with this material [12, 13]. The 30 kV Ga FIB was used for preparing the needle-like shaped sample from the Si isotopic superlattice. A laser-assisted local-electrode atom probe (LEAP3000XSi, AMETEK) with a green laser (wave length: 532 nm) was used for APT analysis. The pulsed laser power and base temperature of the sample were 0.3 nJ and 50 K, respectively. For the reconstruction of APT data, IVAS computer program was used.

detector, but also information of shape of a sample (radius of curvature of start and end of reconstruction calculation, or radius of curvature and shank angle of a sample), and detection efficiency determined by the aperture ratio of MCP hole and electric field [7]. Since these parameters vary according to shape and composition of a sample, it is required to determine most proper parameters for each sample [8]. For example, radius of curvature is usually determined by TEM image before and after APT measurement. However, since especially the sample after APT measurement is not like an ideal sphere but a deformed shape, radius of curvature cannot be uniquely determined. In popular APT reconstruction, radius of curvature was used as the geometric parameter. Since the shank angle, the parameter about the region the signal of APT is detectable, is not the measured value, it is properly adjusted. For example, in case of samples which has some character such as crystal plane or layer thickness, the value of the shank angle are adjusted so that interface between crystal plane would compose their faces or so that each layer thickness would be equal to expected value. This method is usually used in practical APT users. However, this method is reliable only when they had the character information in advance. In other words, the shank angle cannot be decided properly in the sample without the information such as layer thickness. In this study, we propose the method to calculate the value of the shank angle from the shape of sample and the geometric position relationship between the sample and the detector. This makes the reliable APT reconstruction possible even in the sample without the information only if they had SEM or TEM image before APT measurement.

IV. RESULTS AND DISCUSSION

We confirmed how APT data in a real material was reconstructed by using the relationship 1. Figure 2 (a)
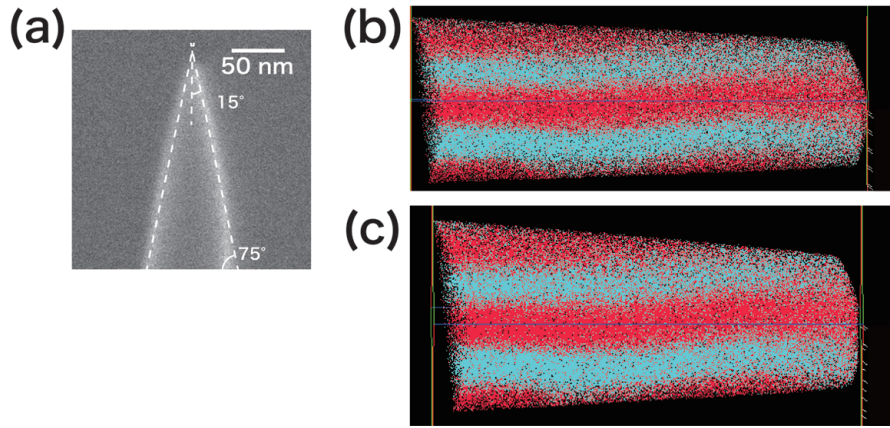
FIG. 2. (a) The SEM image of the needle-like shaped sample made of Si isotopic superlattice. (b) APT reconstruction image by the new reconstruction method. (c) APT reconstruction image by the conventional reconstruction method. Blue dots is ^{28}Si, and red dots is ^{30}Si.
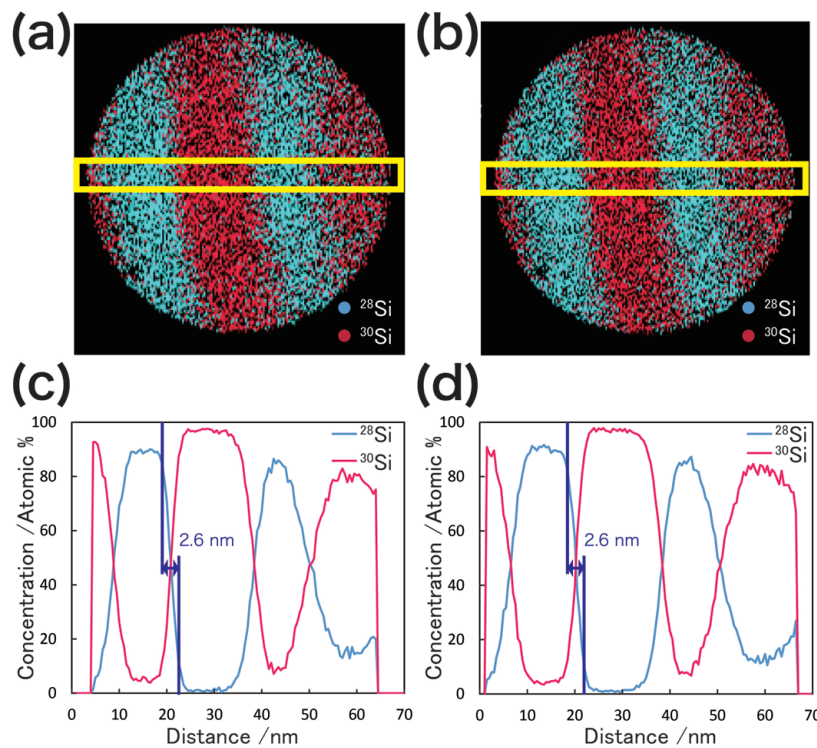

FIG. 3. (a) and (b) show APT reconstruction images at positions from 110 nm to 115 nm from the apex of the samples. (a) Image by the new reconstruction method. (b) Image by the conventional method. (c) and (d) show the distribution of ^{28}Si and ^{30}Si concentration at the yellow area of (a) and (b). The analysis volume was x × y × z = 5 × 70 × 4 nm^3.

shows a SEM image of the needle-like shaped sample fabricated by Ga-FIB. About the sample, radius of curvature was about 50 nm and the half cone angle of the sample was about 15 (= 90 − 75) degree. The complementary angle of the shank angle was calculated as 85.4 degree by the relationship 1. So the value to be inputted as the shank angle was 4.6 degree. Figure 2 (b) shows the APT reconstruction image by using this shank angle value. Figure 2 (c) shows the APT 3D image reconstructed by the conventional method in which the shank angle was adjusted to obtain the best fit between reconstructed and designed layer thicknesses. The value of the

shank angle which yields the best fit is about 7.0 degree. Here, "image compression factor" is the factor to correct the gap between the trajectories of ions field-evaporated from an ideal spherical surface and from an actual sample [14]. The image compression factor greatly depends on the shape of the sample such as the shank angle. In the new method, the values of parameters except the shank angle are not modified from the conventional method because the value of the shank angle is correctly defined and only the difference of the shank angle should be discussed. So Fig. 2 (b) is different from Fig. 2 (c) in the shape of the external form, but it was confirmed that Fig. 2 (b)
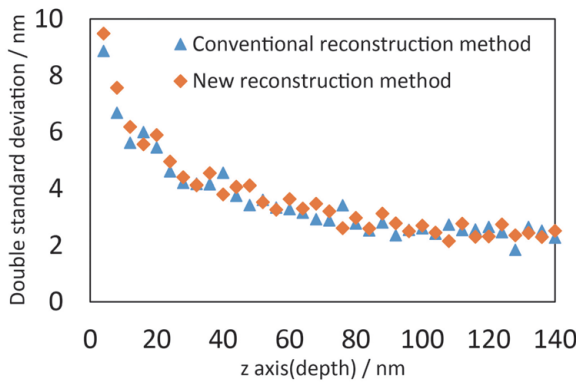
FIG. 4. The relationship between the distance from the apex of the sample and the interface sharpness (double standard deviation). The analysis volume of each depth was x × y × z = 5 × 70 × 4 nm^3.

almost appeared almost equal to Fig. 2 (c).

We considered to what extent the quality of the two APT reconstruction images, Fig. 2 (b) and Fig. 2 (c), were different. Figure 3 (a) and (b) shows the APT reconstruction images at the positions from 110 nm to 115 nm from the apex of the sample. Figure 3 (c) and (d) shows the distribution of ^{28}Si and ^{30}Si concentration at the yellow area of Fig. 3 (a) and (b). In the prior papers, the interface sharpness between layers was often defined as the distance that the concentration of an elements is from 16% to 84% when the concentration was standardized [15]. According to this, the thicknesses of layer boundary in Fig. 3 (c) and (d) were both about 2.6 nm. Therefore Fig. 3 (a) and (b) have almost the equal quality in this point.

Figure 4 shows the relationship between the distance from the apex of the sample and the interface sharpness. In this case, the interface sharpness was evaluated with

double standard deviation of the fitted Gaussian integral function. In the inside of the samples, the interface sharpness in the new method is almost equal to that in the conventional method. Around the apex, the new method gave somewhat the larger values than the conventional method. The depth scale in APT reconstruction image depends on the detection volume. The depth scale becomes smaller when the shank angle becomes larger, in other words, the length of x and y axis becomes longer. As a result, the region damaged by Ga FIB was shifted to the apex in the new method. Therefore this difference seems not so significant, assuming the value of the interface sharpness converges at the shallower position of the depth axis when the shank angle is larger.

As shown above, APT 3D image was reconstructed equivalently to the conventional method, by using only APT measurement data and TEM or SEM image which is always measured in APT analysis, not by using the peculiar value of the sample such as layer thickness.

V.   CONCLUSION

In this study, the new APT reconstruction method was proposed, and APT reconstruction image equivalent to the image in the conventional method can be obtained. This means that a reliable 3D image can be reconstructed in the new reconstruction method for even samples without internal length reference if there is a SEM or TEM image of the samples before APT measurement.

ACKNOWLEDGMENTS

[1] M. Fuechsle, J. A. Miwa, S. Mahapatra, H. Ryu, S. Lee, O. Warschkow, L. C. L. Hollenberg, G. Klimeck, and M. Y. Simmons, Nat. Nanotechnol. **7**, 242 (2012).
[2] D. N. Seidman, Annu. Rev. Mater. Res. **37**, 127 (2007).
[3] T. Kelly and M. Miller, Rev. Sci. Instrum. **78**, 031101 (2007).
[4] B. Deconihout, F. Vurpillot, B. Gault, B. Da Costa, M. Bouet, A. Bostel, D. Blavette, A. Hideur, G. Martel, and M. Brunel, Surf. Interface Anal. **39**, 278 (2007).
[5] B. Gault, F. Vurpillot, A. Bostel, A. Menand, and B. Deconihout, Appl. Phys. Lett. **86**, 094101 (2005).
[6] T. F. Kelly, D. J. Larson, K. Thompson, R. L. Alvis, J. H. Bunton, J. D. Olson, and B. P. Gorman, Annu. Rev. Mater. Res. **37**, 681 (2007).
[7] B. Gault, F. Geuser, L. T. Stephenson, M. P. Moody, B. C. Muddle, and S. P. Ringer, Microsc. Microanal. **14**, 296 (2008).

[8] R. Gomer, *Field emission and field ionization* (Harvard University Press, Cambridge, 1961).
[9] T. Kojima, R. Nebashi, K. M. Itoh, and Y. Shiraki, Appl. Phys. Lett. **83**, 2318 (2003).
[10] Y. Shimizu and K. M. Itoh, Thin Solid Films **508**, 160 (2006).
[11] D. J. Larson, T. J. Prosa, B. P. Geiser, and W. F. Egelhoff Jr., Ultramicroscopy **111**, 506 (2011).
[12] Y. Shimizu, Y. Kawamura, M. Uematsu, K. M. Itoh, M. Tomita, M. Sasaki, H. Uchida, and M. Takahashi, J. Appl. Phys. **106**, 076102 (2009).
[13] Y. Shimizu, Y. Kawamura, M. Uematsu, M. Tomita, T. Kinno, N. Okada, M. Kato, H. Uchida, M. Takahashi, H. Ito, H. Ishikawa, Y. Ohji, H. Takamizawa, Y. Nagai, and K. M. Itoh, J. Appl. Phys. **109**, 036102 (2011).
[14] R. Newman, R. Sanwald, and J. Hren, J. Sci. Instrum. **44**, 828 (1967).
[15] M. Karasawa, M. Fujii, M. Morita, S. Ishimura, N. Mayama, H. Uchida, Y. Kawamura, K. M. Itoh, and M. Owari, Surf. Interface Anal. **46**, 1200 (2014).